



Phase change material's (PCM) impacts on the energy performance and thermal comfort of buildings in a mild climate



Barilelo Nghana^{*}, Fitsum Tariku

Building Science Centre of Excellence, British Columbia Institute of Technology, UK

ARTICLE INFO

Article history:

Received 1 October 2015
Received in revised form
22 January 2016
Accepted 23 January 2016
Available online 29 January 2016

Keywords:

Phase Change Material
Thermal comfort improvement
Energy savings
Thermal stabilization
Peak shaving

ABSTRACT

The current residential buildings are of light weight construction. As such, they tend to frequent indoor air temperatures fluctuations and have been proven detrimental for thermal comfort and mechanical system energy consumption. This is reflected in the energy consumption statistics for residential buildings. More than 62% of the building energy use is towards maintaining comfortable indoor conditions. Phase change materials (PCM); a latent heat thermal storage material, have the potential to increase the thermal mass of these buildings without drastically affecting the current construction techniques. In this paper, the potential of phase change materials is investigated through numerical and experimental studies. The field experimental study is conducted using twin side-by-side buildings exposed to the same interior and exterior boundary conditions, and EnergyPlus, after being benchmarked with the experimental results, is used for the numerical study. The numerical study is carried out for an existing residential apartment unit with particular emphasis on the effects of different design parameters such as orientation and window to wall ratio. Preliminary analyses of experimental data show that phase change materials are effective in stabilizing the indoor air by reversing the heat flow direction. In fact, the indoor air and wall temperature fluctuations are reduced by 1.4 °C and 2.7 °C respectively. Following, benchmarking of the numerical simulation shows confidence levels in predicting the interior conditions since discrepancies between experimental data and numerical data are within tolerance limits of the measuring device. Further, from the analysis of the numerical data, phase change material is effective in moderating the operative temperature but does not translate to significant thermal comfort improvement when evaluated over a night time occupancy regime in the summer. On the contrary, PCM is effective in lowering the heating energy demand by up to 57% during the winter condition.

© 2016 Elsevier Ltd. All rights reserved.

1. Introduction

The residential building construction industry in North America is dominated by lightweight structures which have low thermal mass. The low inertia buildings tend to frequent indoor temperature fluctuations and are prone to overheating in the summer. As a result, maintaining favorable interior conditions for thermal comfort requires significant amount of energy usage in active heating and cooling systems. In fact, according to Natural Resources Canada (NRCAN), about 65% of energy consumption in buildings is attributed to space heating and cooling as of 2013 [1]. The temperature fluctuations and overheating experienced in these low inertia

buildings can be reduced by integration of thermal mass in the building envelope. The idea is that, by improving the thermal inertia of these buildings, excess heat and cold can be stored thereby reducing the instantaneous cooling and heating loads experienced in these buildings and consequently reducing the energy consumption of mechanical heating and cooling systems.

Phase change materials (PCMs) provide a feasible means of integration of thermal mass in these low inertia buildings without requiring a drastic change in the current construction practice. PCMs are latent thermal storage materials that possess larger heat storage capacity per unit volume than typical building materials [2]. They store heat by a change of phase from solid to liquid as the ambient temperature increases above their melting point and release the stored heat as the ambient temperature drops below their freezing point. The benefits of integration of PCM in the building envelope have been researched for some time now and are

^{*} Corresponding author.

E-mail address: nghanabarilelo@yahoo.com (B. Nghana).

well documented. This cyclic process stabilizes the interior conditions that have been shown to provide benefits in terms of energy conservation and thermal comfort improvement. However, the effectiveness of the incorporation of PCM in buildings for thermal inertia improvement is hinged mainly on the climatic characteristics with respect to the solar radiation, diurnal temperature swing and outdoor temperature [3]. As such, the PCM properties; melting temperature and range, latent heat storage capacity and thermal conductivity, have to be optimized specific to the climate [4]. The building characteristics such as the building envelope design, glazing area and orientation, shading structure, occupancy behavior, HVAC design, building operation schedule are also important since the building design determines the shield of the interior environment from the exterior climate and could be optimized to create favorable conditions to extract more PCM benefits.

Investigations as to the suitability of PCMs in different climates have yielded promising results. In tropical climates, up to 2.5hr and 18% phase shift and peak cooling load reduction is observed as well as a reduction in the cooling load in the range of 29%–100% [5,6]. In Mediterranean climate [7–12], demonstrated that incorporating PCM can reduce daily indoor air peaks in the range of 1 °C–2.5 °C, decrease thermal amplitude in the span of 2 °C–5 °C, increase night time temperatures up to 2.1 °C, and shift peaks in the limits of 4 °C–8 °C. As a result, the energy needs are impacted such that the cooling energy savings in the range of 29%–100% and up to 16% heating energy savings is attained while still improving comfort by 10.7%–57%. In warm temperate [5,13–26], showed that PCM integration in buildings can damp the peak air and wall surface temperature in the range of 1 °C–4 °C and increase the night time temperature in the limits of 2 °C–2.3 °C. Also, peak load shifting in the span of 1.5 hr–11 hr, cooling load lowering in the limits of 25%–35%, 9.4%–81% cooling energy savings, –13.4%–2.9% total energy savings, and payback in the bounds of 6.38 years–11 years was realized. Additionally, up to 10% reduction of yearly discomfort hours, 11.4% reduction in cooling electricity cost and 6.9% heating energy savings is attained. For continental climates [3,5,16,27–35], showed that PCM can help lower; heat flux by 12%–38%, peak cooling load by 8.6%–91.8%, annual cooling load by 9.28%–45%, heating energy by 6%–12%, cooling energy by 13.6%–76%, peak air temperature by 0.85 °C–4 °C, thermal amplitude by 1.15 °C–2 °C, and cooling electricity cost reduction by up to 12.76%. As well, a phase shift in the range of 2.5 hr–3 hr is achieved and a 3–5 years payback is achievable. In dry (Arid and Semi-Arid) climate [36–40], showed that with PCM one can achieve cooling load reduction in the limits of 24.3%–100%. Likewise, the peak heating load, peak cooling load and peak surface temperature can be lowered by up to 35.4%, 40% and 2 °C respectively. Up to 3 °C night time temperature increase and payback time of 10.5 years can be achieved. Under maritime temperate (mild) climatic conditions [41–48], demonstrated a 3.2 °C–4.7 °C thermal amplitude decrease, 1.5 °C–11 °C trough temperature increase, 2.2 °C–20 °C peak attenuation, 21%–100% heating energy savings and up to 34.5% cooling energy savings.

The positives to incorporating PCM in buildings is clearly seen regardless of the climatic conditions, however, PCM is more cost effectively integrated in mild climates as in some cases specialized system were designed in harsher climatic regions in order to reap the PCM benefits [6,23,32,40]. That being said, the performance of PCM in mild climate has not been thoroughly investigated, most of the experimental analysis were carried out in small test facilities that do not reflect internal loading in actual buildings [42,46–48]. The numerical simulations were either not benchmarked, benchmarked with unreliable data, or not unsatisfactorily matched [41,46]. Others were carried out under simulated exterior conditions [47] or displayed limited variable exploration such as

occupancy behavior and building characteristics [44,45]. In this paper, a holistic approach is adopted in investigating the potential for application of PCM in residential buildings such that the effect of occupancy and changing building characteristics are considered. This study is carried out for a mild climate like Vancouver, BC, with focus on thermal comfort and energy consumption improvements. The secondary objective of this work is to provide experimental data for numerical simulation validation. This research is structured in three phases. The first phase involves experimentally monitoring two test buildings; Whole-Building Performance Research Laboratory (WBPR) [49], for which one is equipped with PCM and the other serving as the reference building. The aim of this phase is to understand the performance in small scale building and also generate data for benchmarking of the numerical model, EnergyPlus. In the second phase, the numerical simulation model is benchmarked against the experimental data from phase 1. Lastly, the impact of PCM on the energy, thermal comfort and peak load of an existing residential apartment unit and the effects of different design parameters such as orientation and window to wall ratio are investigated in mild costal climate using the benchmarked numerical model.

2. Experimental study

In the experimental study, two buildings located side by side each other; with and without PCM, are monitored synchronously for the month of September, 2014. The two experimental facilities are exposed to identical boundary conditions with residential occupancy simulated by internal heat source and ventilation that meet ASHRAE 62.2 requirements to imitate passive cooling by opening the windows. The experimental facilities are instrumented to monitor the indoor air and outdoor climatic conditions, ventilation rates and internal heat transmission through the building envelope. Data from the experimental period is analyzed to understand thermal behavior under different seasons based on the outdoor temperature and solar trend.

2.1. Overview of the experimental facility (WBPR)

The two test facilities are situated side-by-side as depicted in Fig. 1 and are located in British Columbia Institute of Technology, BCIT, Burnaby campus (123° Longitude and 45° latitude). Both buildings are designated names consistent with their relative position on the site; North and South, and are positioned such that the surrounding buildings and trees do not interfere with the external climate [49]. The length, width, and height dimension as 16' × 12' × 8'. The mechanical rooms located at the north-west corners of both test buildings. The mechanical rooms house the air handling unit, data acquisition systems and instrumentation. The mechanical rooms are separated from the test spaces by an interior partition (Table 1) with doors linking the exterior and the interior space. The doors are metal with height and width dimensions of 8' × 4'. Both buildings have HSS steel skeleton-frame structure and insulated slab on grade foundation with walls and roofs constructed with 2" × 6" wood studs and 2" × 12" wood joists respectively. The walls and roofs are fiber batt insulated and have a gypsum wallboard finish. Table 1 shows a complete description of the wall, roof and floor assembly. Both buildings have two windows in the north and south wall orientation. The windows are vinyl framed and air filled with height and width dimensions of 4' × 3' respectively. As well, some of the floor area is take up by the mechanical room in both buildings. The mechanical system is highly flexible and can be configured to provide heating, cooling, ventilation, humidification, and dehumidification. Exterior climate is monitored by an onsite weather station.



Fig. 1. From left: North (with PCM) and South (without PCM) Test Building.

Table 1

Building envelope construction details.

Component	Assembly detail	
wall	Exterior Wall <ul style="list-style-type: none"> • 5/6" fiber cement cladding • ¼" air cavity • Spun bonded polyolefin sheathing membrane • ½" Plywood sheathing board • 2" × 6" Wood stud w/R20 fiberglass batt insulation • 6mil Polyethylene film • ½" gypsum drywall 	Interior Wall <ul style="list-style-type: none"> • ½" Plywood sheathing board • 2" × 4" Wood stud w/R14 fiberglass batt insulation • ½" Plywood sheathing board • ½" gypsum drywall
Roof	<ul style="list-style-type: none"> • 2 ply SBS modified bitumen • Plywood sheathing • Air gap • 2" × 12" wood joist w/R40 glass fiber insulation • 6 mil polyethylene sheet 	
Floor	<ul style="list-style-type: none"> • Gypsum drywall • 12" concrete slab • 3" Rigid Insulation (EPS) • 6 mil Polyethylene film 	

2.2. Experimental setup

2.2.1. PCM installation

For this research, BioPCM is selected over paraffin based PCM based on comparison of the thermophysical properties, availability and safety (less flammable). For the same melting temperature, the BioPCM has almost double the latent heat storage capacity allowing for a greater potential for thermal stabilization. To be more specific, the Latent heat for the BioPCM and Paraffin based PCM is 200 kJ/kg and 107.5 kJ/kg respectively. The other thermophysical properties of the BioPCM are outlined in Table 2.

The South building is designated the control building while the North building is modified with the BioPCM (Fig. 2). To install the BioPCM in the exterior walls, the gypsum wall board is removed and the BioPCM is fitted squarely between the studs such that the flanges rest on the wood studs. The flanges are stapled to the wood studs and taped to restore integrity of the polyethylene air barrier, and then the gypsum is reinstalled.

2.2.2. Instrumentation

The experimental facilities are fitted with sensors to collect data for the thermal characterization of the impact of the PCM on the indoor environment. The sensors are positioned with consideration



Fig. 2. PCM installation behind gypsum drywall.

given to the effects of thermal stratification, wall orientation, spatial wall temperature variation, and location of window and door openings. The parameters being measured are the interior air temperature, surface temperatures (interior, exterior and between

Table 2

Thermophysical properties of BioPCM phase change material.

Melting point (°C)	Density (kg/m ³)	Specific heat (kJ kg ⁻¹ °C ⁻¹)	Latent heat (kJ/kg)	Thermal conductivity (W m ⁻¹ °C ⁻¹)
23	860	2.1	200	0.2

wall components), heat flux, and the external climatic data. Additionally, the mechanical system is equipped with sensors laid out at different locations to measure local temperature, relative humidity and air flow rate.

The interior air temperature measurement is by means of multiple relative humidity and temperature (RH-T) sensors (L: 71 mm, D: 12 mm, accuracy: $\pm 0.6\text{ }^{\circ}\text{C} \pm 3\%$) positioned at three locations in both buildings referenced based on their relative distance from the air supply inlet. One closest to the air supply inlet is 5 ft from the ground such that it is not affected by sudden opening and closing of the door, the other farthest from the air supply inlet is 2 ft from the ground and is positioned such that the solar radiation from the window does not affect the readings of the RH-T, and three at the middle of the room are 2 ft, 5 ft and 7.7 ft above the ground.

The surface and internal temperatures are measured by means of Type T thermocouples with an accuracy of $\pm 1\text{ }^{\circ}\text{C}$ and a measurement range of -270 to $400\text{ }^{\circ}\text{C}$. Five thermocouples are installed in the roof between the two stacked 6" fiber batt insulations. One is centrally positioned while the other four thermocouples are positioned at each corner of the roof. Each of the four thermocouples is 2 ft square from the projected interior wall corners. This was to determine the spatial variation of the temperature across the roof. Thermocouples are distributed along the height of the foundation wall since the foundation wall was exposed to varying boundary conditions. The thermocouples are symmetrically positioned on all four foundation wall orientations (north, south, east, and west) and measure 8 in, 12 in and 20 in from the top of the wall and coincide with the meeting point of the foundation wall and finish grade, projected interior depth of the concrete slab and projected exterior depth of the concrete slab respectively. Six thermocouples are arranged underneath the concrete floor and footing such that they symmetrically divide the slab into four quadrants this is to account for edge effects and ground coupling. One is centrally positioned, all four orientations have one which is 9.5 in from the edge of the concrete footing, however, the east and west have an additional one that is about 2 ft inwards for spatial temperature variation within the actual test space. There is an additional thermocouple at the middle underneath the extruded polystyrene insulation. One thermocouple is located on each exterior wall orientation. The positioning of the thermocouple on the north and south mirror each other and is 24 in from the end of the mechanical room and 56 in above the ground. The dimensions are referenced for the north wall. Same applies for the east and west wall orientation. There are 23 thermocouples on the interior wall surfaces; five on the North wall, 11 on the south (Fig. 3), three on the east wall, and four on the west wall. The sensors are arranged to account for thermal bridging and wall edge effects. Fig. 4 shows the layout of the sensors on each of the wall orientations.



Fig. 3. Sensor layout on the south wall.

The heat flux is measured by heat flux transducers ($44.5\text{ mm} \times 44.5\text{ mm} \times 2.8\text{ mm}$, error $\leq \pm 5\%$, HFM) that are centrally positioned at the undisturbed area of the four exterior wall orientations, such that it is directly above a PCM block. The heat flux transducers are 6 ft measured from the concrete slab. The data acquisition systems for the north and south experimental facilities are configured to collect data within 5 min intervals. The data collected is converted and written in a CSV format via a Vee program. The data collected is stored on site and can be retrieved easily.

The outdoor climatic conditions to which the experimental buildings are exposed to, including the temperature, relative humidity, wind speed and direction, solar radiation and rain loads are measured by an onsite weather station. The weather station is located far from any obstruction from nearby building structures or terrestrial bodies. The data acquisition system is configured to collect and read data per 1 min interval.

2.2.3. Building operation

The HVAC system is configured in such a way that the building is maintained between $20\text{ }^{\circ}\text{C}$ and $27\text{ }^{\circ}\text{C}$. The occupancy behavior is captured in this ventilation scheme, such that the occupants tend to open the windows to allow some fresh air when the space is unoccupied and vice versa. The minimum ventilation rate is derived from minimum requirements for ventilation as per ASHRAE 62.2. The maximum ventilation of 45 cfm is an imposed constraint such that too much heat is not added to the fresh air that is being introduced into the space. The ventilation algorithm implemented in the experiment is given below:

If $\text{OAT} > \text{IAT}$, $\text{CFM} = 7.5$

Else, $\text{IAT} > 27$, $\text{CFM} = 45$

$\text{IAT} < 20$, $\text{CFM} = 7.5$ & switch on supplemental heating

$\text{IAT} \geq 20$ & ≤ 27 , CFM is proportional between 45 & 7.5

Heat addition to the space as a result of human activity is simulated by light bulbs rated at 72 W. The light bulb is centrally positioned in the test space and is scheduled to come on at 7am and go off at 7pm. This is based on the reasoning that people tend to be more active during the day.

2.3. Experimental results and discussions

The field experiment was conducted from September 2nd to October 8th, 2014. This period is characterized by falling outdoor temperature as shown in Fig. 5. For the first 10 days of the experiment the average peak outdoor air temperature is about $23\text{ }^{\circ}\text{C}$, with maximums of up to $29\text{ }^{\circ}\text{C}$. The last few days show a reduced peak outdoor air temperature. In fact, the maximum peak outdoor air temperature observed for the last ten days of the field experiment is $22\text{ }^{\circ}\text{C}$ and an average of about $19\text{ }^{\circ}\text{C}$. The same trend is observed for the solar intensity, for the first 10 days, an average peak solar radiation intensity of 653 W/m^2 is calculated, while that for the last 10 days of the field experiment is 435 W/m^2 . As such, excerpts are taken from different times over the course of the experimental period to analyze the impact of the PCM on the indoor thermal environment for consecutive hot days and consecutive cool days. September 10th to 16th is representative of typical hot days and September 22nd to 28th is representative of typical cool days (Fig. 6).

Fig. 7 depicts the behavior of the PCM under typical hot days. It can be seen that the indoor air temperature profiles for the North

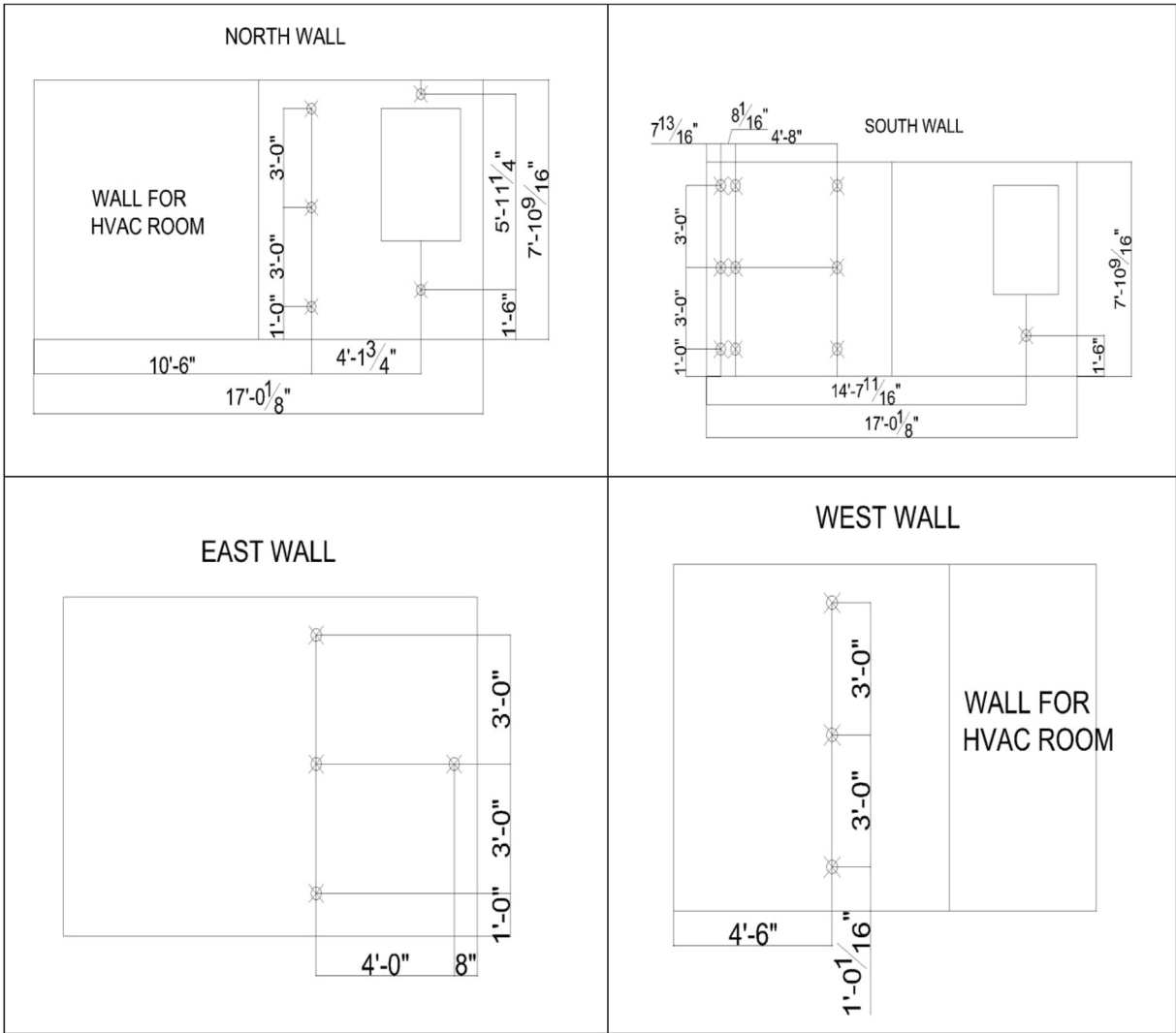


Fig. 4. Thermocouple layout for the different wall orientations.

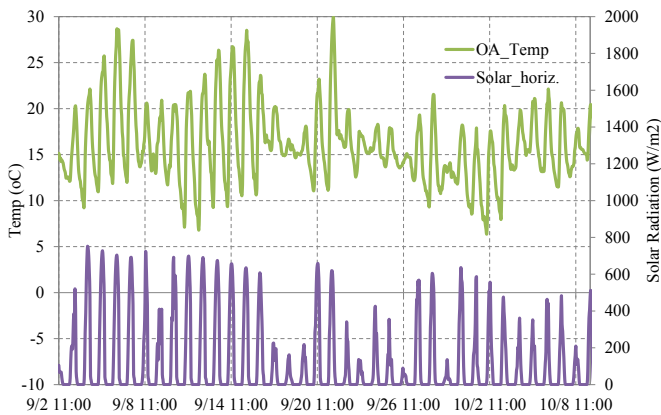


Fig. 5. Measured weather data during the field testing.

and south buildings are different. In the North building, the temperature amplitudes are lower than in the south building. The north building experiences lower indoor air temperature during the day and higher temperatures at night. Both curves intercept each other

at a point during the day when the BioPCM is neither storing nor releasing heat. In fact, for the hottest day, September 15th, 0.6 °C peak indoor temperature attenuation is observed (Fig. 9) and 0.8 °C night time temperature increase is observed. This is attributed to the heat storage and release process of the BioPCM.

This phenomenon is further explained with the heat flux data for the day in consideration (Fig. 10). Only the heat flux for the west wall is shown for clarity although data was collected for all wall orientations. During the day when the outdoor temperature is high, the building is gaining heat. This is reflected by the negative heat flow values for the south building. However, for the north building, this is not the case. The positive heat flow values indicate that the direction of heat flow is reversed for the same period of the day, indicating that the PCM in the walls is absorbing excess heat from the space. The PCM being a latent heat storage material stabilizes the temperature during the charging process and hence the reason for the lower indoor temperature. As the outdoor temperature drops, the south building is losing heat to the outdoors, which is reflected in the positive heat flow values. However in the north building the negative heat flow indicate that the building is gaining heat, which in fact is indicating that the PCM is releasing the heat stored during the day and hence the higher indoor air temperatures during the night time.

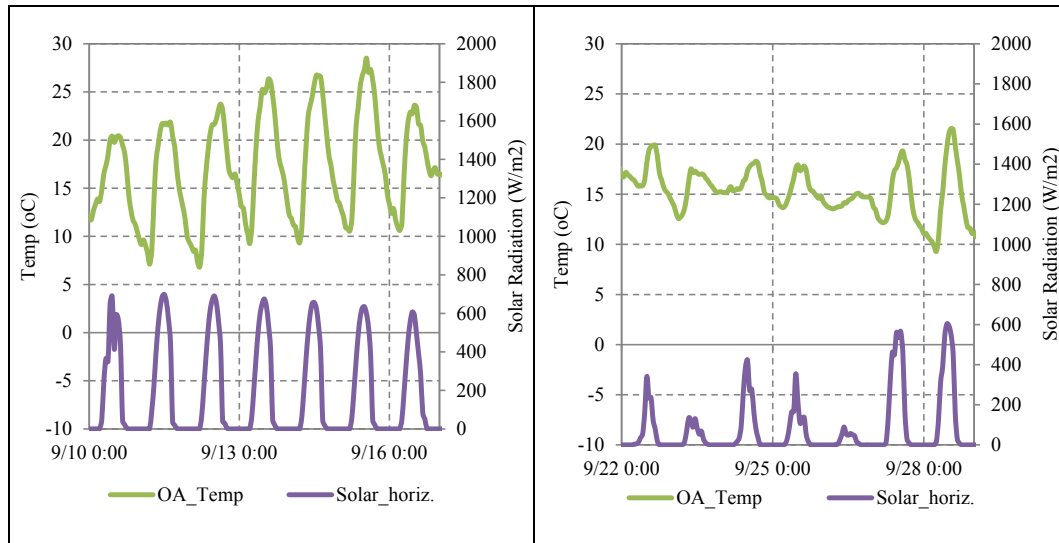


Fig. 6. Weather Data representative of typical hot (Left) and cold (Right) days.

A further enhancement of the thermal comfort attributed to the BioPCM can be seen in the wall surface temperature profiles (Fig. 11). Again, only the west wall temperature evolution is shown for clarity. The potential for the BioPCM to stabilize the wall surface temperature can clearly be seen. For the day under consideration, the thermal amplitude for the South building is 4.6 °C while that of the North building is 2.4 °C, which is a 2.2 °C decrease in the temperature amplitude. In fact, up to 1.5 °C peak attenuation during the day and 1.2 °C night temperature increase is achieved in the North building. The wall temperature stabilization of the BioPCM indirectly impacts the thermal comfort by directly influencing the mean radiant temperature making the space to feel cooler and more comfortable.

As the outdoor temperature gets cooler, the effect of the BioPCM in terms of thermal comfort improvement is not as pronounced as in elevated outdoor air conditions. Fig. 8 depicts the behavior of the

PCM under relatively cooler days. This is expected since the indoor temperature does not get as high as the melting temperature of the PCM. In fact, for the coldest day, September 26th, the temperature amplitude in both buildings is identical despite the offset of about 0.15 °C between the indoor temperature profiles (Fig. 12). The slight offset is attributed to the higher thermal inertia of the north building. It is interesting to note that although the temperature does not get as high as the theoretical melting point of the BioPCM, some activation of the PCM is observed (Fig. 13). Although the heat flow stays positive, during the day, the heat flow in the north building is slightly more positive indicating that the PCM is absorbing and at night the heat flow in the south is less positive indicating that some heat is being released into the space. This asserts that the theoretical melting temperature of the BioPCM deviates from the actual melting point. The inability of the PCM to enhance the thermal comfort is further stressed in Fig. 14, as the

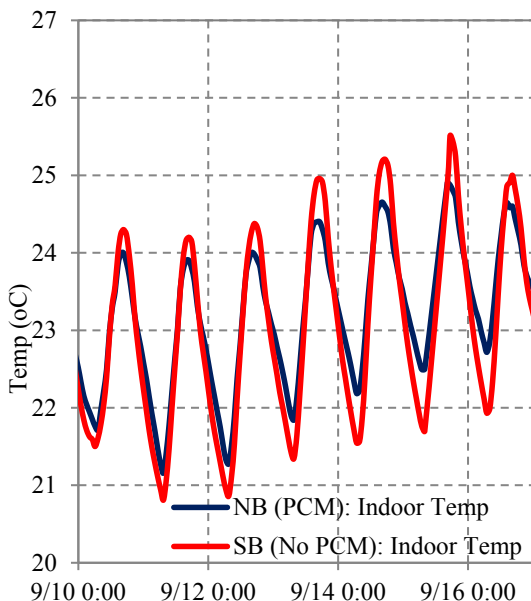


Fig. 7. Indoor air temperature comparison of both buildings on typical hot days.

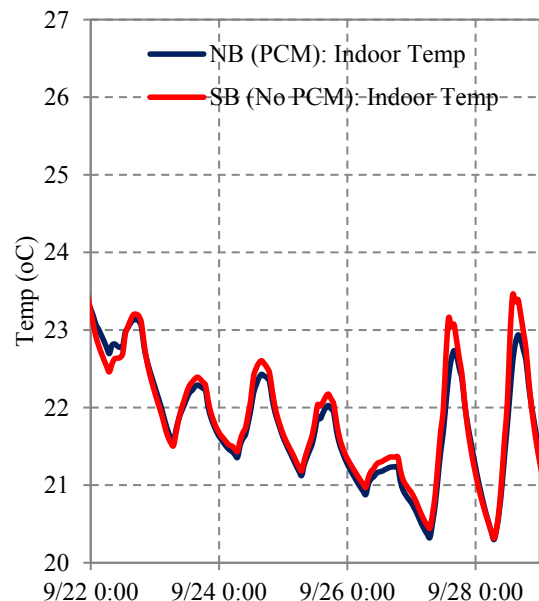


Fig. 8. Indoor air temperature comparison of both buildings on typical cold days.

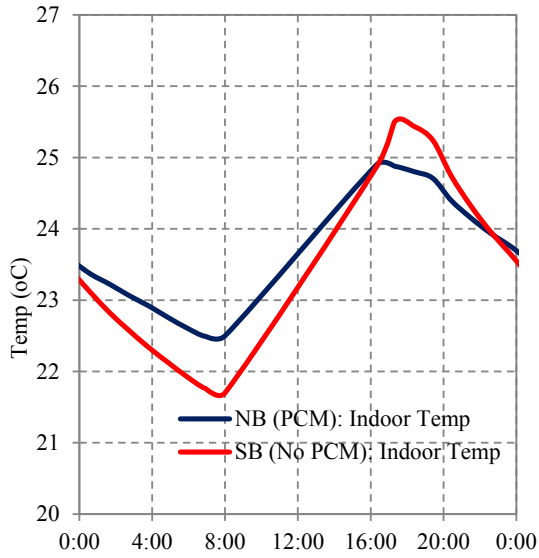


Fig. 9. Indoor air temperature comparison of both buildings on September 15th.

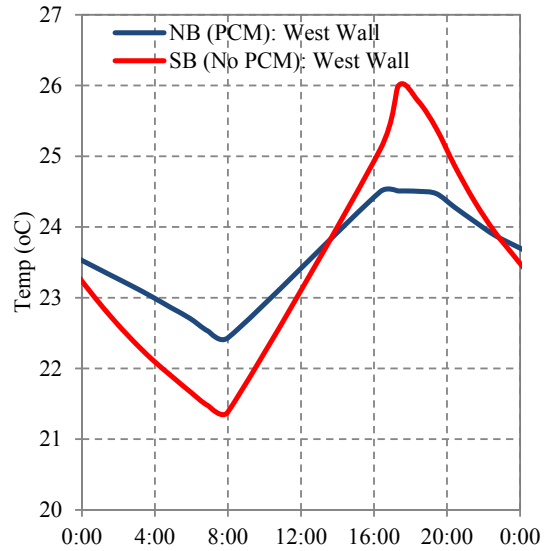


Fig. 11. Interior wall surface comparison of both buildings on September 15th.

wall surface temperatures in both buildings are very identical.

From the field experiment data analysis, the impact of PCM on the thermal comfort of buildings under a mild climate like Vancouver, BC, can clearly be seen. This is more pronounced in the summer because of the elevated peak outdoor air temperature conditions. By simulating residency with ventilation, ideal thermal conditions and heat gains experienced in typical residential buildings is realized. This combined with the moderate climatic conditions enabled the incorporation of PCM with melting temperature of 23 °C, which is within the temperature range for thermal comfort as specified by ASHRAE [50]. This speaks to the conduciveness of the climate of Vancouver for the application of PCM in the building envelope and the ability of the PCM to provide passive cooling. In fact, up to 1.5 °C peak attenuation and 1.2 °C night time temperature increase is observed. The same cannot be said in the colder period, since the PCM is barely activated.

However, the offset of the indoor air temperature when both buildings are compared may signal a potential for energy savings as the heat loss drive across the building envelope is reduced.

3. Benchmarking of energyplus for buildings with PCM

In this section, EnergyPlus 8.1 is benchmarked with the experimental data earlier presented. EnergyPlus is chosen as the numerical simulation software mainly because of its readily availability. Additionally, it's highly object oriented user input format allows for simulation of customized heating, ventilation and air conditioning system configurations and advanced building materials like phase change materials [51]. The simulation of phase change materials is achieved by dynamically varying the thermal properties based on a user input enthalpy–temperature relationship in the conduction finite difference heat balance solution module. The benchmarking is carried out in increasing levels of

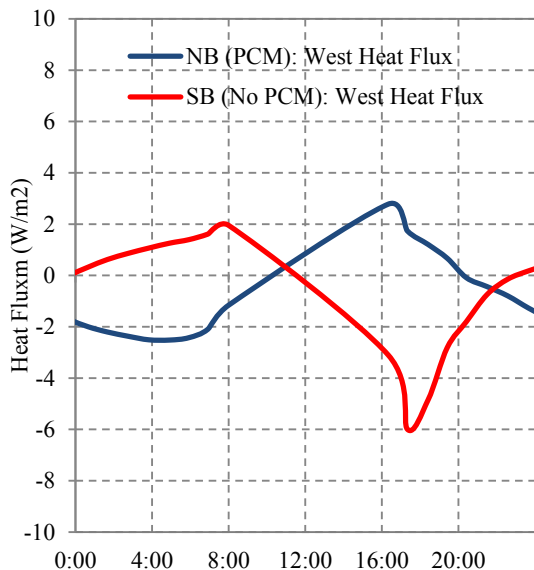


Fig. 10. Heat Flux comparison of both buildings on September 15th.

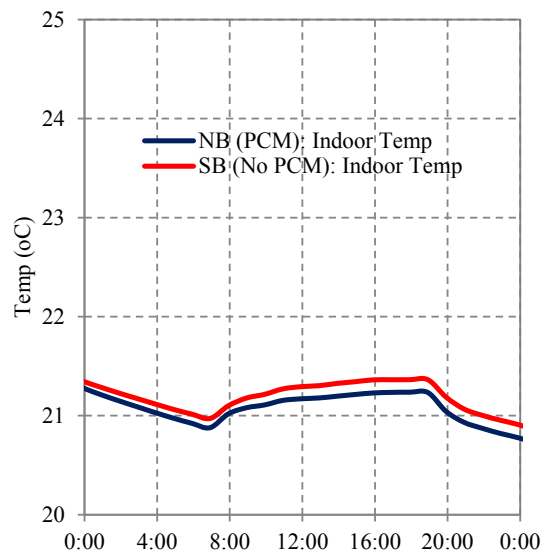


Fig. 12. Indoor air temperature comparison for both buildings on September 26th.

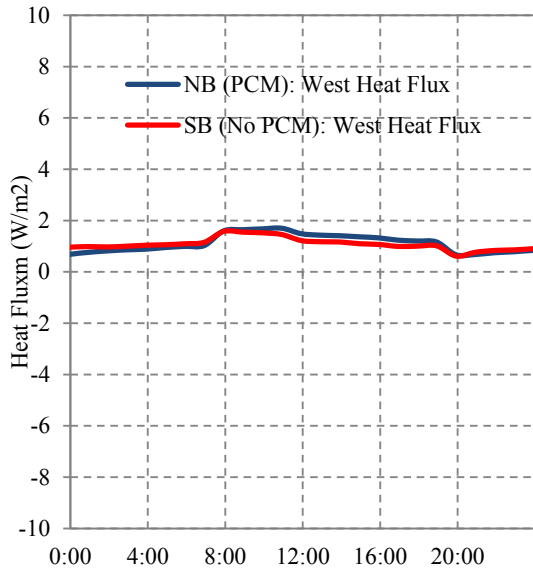


Fig. 13. Heat flux comparison for both buildings on September 26th.

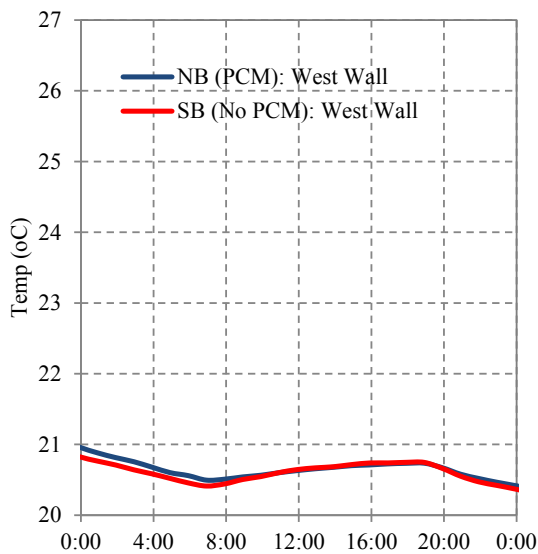


Fig. 14. Interior wall surface comparison for both buildings on September 26th.

complexity: first, the South building (without PCM) and then, the North building (with PCM). The simulation is designed to duplicate the experimental setup described earlier and the results matched numerically.

3.1. Simulation inputs

The inputs for the simulation reflect the construction and operation of the WBPR L i.e North and South building having identical geometry, dimensions, orientations, envelope characteristics, and building operation. Both buildings have two zones, actual test space and the mechanical room, having floor areas of 14.54 m² and 3.3 m² respectively. Both zones are separated by an R 10 wall assembly; regarded as an interior partition (Table 1) and a metal door (R 1.53) while the exterior walls and roof have a thermal resistance of approximately R 13 and R 30 respectively. Refer to Table 1 for a more detailed description of the building envelope characteristics. The materials are layered as described in Table 1 with material properties adopted from ASHRAE handbook of fundamentals 2013 [52]. Table 3 highlights the material properties adopted for the simulation. The two windows in the test space have a U-value of 2.612 W/m²K and a solar heat gain coefficient of 0.63.

Further, the enthalpy–temperature relationship describing the dynamic thermal properties of the phase change material is described in Fig. 15 below. The emissivity of the interior and exterior wall surface is 0.7 and 0.9 respectively. That of the roof is 0.9. The absorptivity of the interior and exterior wall surface is 0.75 and 0.6 respectively. That of the roof is 0.9. The interior and exterior wall surfaces are assumed medium smooth with inside and outside surface coefficients calculated dynamically using the simple natural and simple combined convection algorithm.

The light source simulating occupancy is assumed 100% radiative. The radiant heater is modelled as an electric equipment having a rated power output of 1500 W and is assumed 100% radiative. The control of the radiant heater is achieved through the Energy Management System in EnergyPlus. The contribution of the heat generation in the mechanical room to the heat balance in the test space is accounted for by directly inputting the measured indoor air temperature from the field testing. This is done via the Ideal Loads Air System in EnergyPlus such that the heating and cooling set-points are the indoor air temperature accurate to the 4th decimal place. For example if the measured air temperature at a certain time is 27 °C, the heating and cooling setpoint for the ideal loads air system will be 26.9999 °C and 27.0001 °C respectively. The measure ground temperature at the insulation to ground interface is directly input into the simulation as boundary condition. This is done via the Surface Property: Other side Coefficients in EnergyPlus. Edge effects are accounted for by having different temperatures for the center and edges of the slab on grade construction. The heat generated in the mechanical room interferes with the thermal condition of the supply air. For this reason the measure condition of the supply air at the diffuser is a simulation input. This is done by creating a zone far away from the WBPR L such that it does not interfere with the exterior conditions and imposing the indoor air temperature as the supply air temperature using the Ideal Loads Air System. The conditioned air is then exchanged with the air in the test space via the Zone Cross Mixing in EnergyPlus. The buildings

Table 3
Material properties.

Materials	Conductivity (W/m-K)	Density (kg/m ³)	Specific heat (J/kg-K)
Fiber cement	0.245	1380	840
Plywood Sheathing	0.1	500	1500
Composite 2 × 6 Wood Stud R19	0.05	93.84	1006
Gypsum	0.16	625	870
Extruded Polystyrene	0.049	40	1500
Composite 2 × 4 Wood Stud R11	0.05	119.63	1048
Concrete	1.95	2240	900
BioPCM	0.2	235	1970

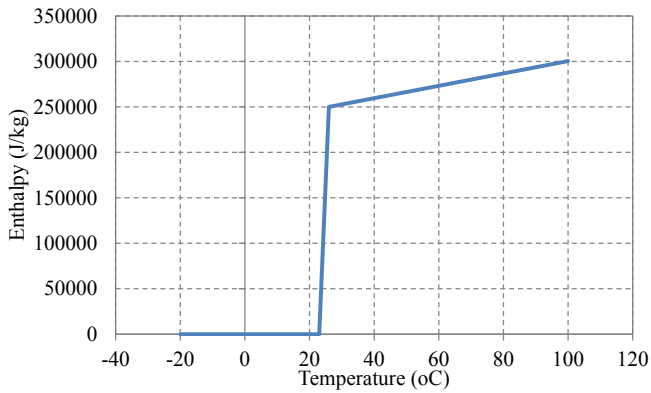


Fig. 15. Enthalpy vs Temperature curve for BioPCM.

are simulated with a weather file modified with the locally measured weather data. The initial condition of the simulation is imposed via the Ideal Loads Air System based on the measured indoor air temperature for a period of three days after which the indoor air temperature is allowed to float based on the interaction with the exterior climate and boundary conditions. The simulation time step is 1 min and default space discretization factor.

3.2. Experimental benchmarking results

The simulation is carried out from September 9th to September 30th 2014. EnergyPlus predicts the indoor air temperature for the two building having different thermal inertia and is compared with measured indoor air temperature data from the field experiment. Fig. 16 shows the indoor air temperature prediction of the Energyplus compared with the field measurements for the south building (without PCM). The result from the field experiment is shown in red and that of the EnergyPlus simulation is shown in blue. Notice that for the first three days, the experimental data and the simulation results are accurately matched. This period corresponds to the period during which the initial condition is still being imposed. The indoor air temperature is then allowed to float and some discrepancies between the simulations and field data. In general, the indoor air temperature peaks are better matched than the crests. This implies that the building is losing more heat in the simulation than the field experiment. That being said, the maximum deviation over the simulation period is 0.6 °C and

considering that this is within the tolerance limits for the RH-T's used in the field experiment, it is concluded that there is no measurable difference and the agreement between the EnergyPlus simulation results and the measured data is satisfactory. With the incorporation of the PCM in the building envelope of the North building, one can immediately notice the damping of the temperature amplitude attributed to the heat storage and release capability of the PCM (Fig. 17). More important is the agreement between the simulation results and the measure data. An even better agreement is achieved. To be more specific, the maximum deviation between the two plots is 0.4 °C, which is within tolerance limits of the RH-T's used in the field experiment. Hence, it is concluded that there is no measurable difference between the two plots. In all cases, EnergyPlus was able to predict the indoor air temperature profiles within reasonable amount of accuracy, hence the results from the numerical simulation can be relied upon for further analysis.

4. Numerical study of PCM in an existing apartment unit

In the numerical study, a two bedroom apartment is simulated for a year under real operating conditions such that the occupancy schedule and appliance usage are considered. The window to wall ratio of one of the bedrooms is modified to depict a room with low solar influx. This is done to investigate the impact of solar exposure to PCM performance. Other building characteristics such as the building global orientation are changed for further analysis on the solar exposure effect. Output from the simulation is analyzed for thermal comfort enhancement in the summer and energy savings in the winter.

4.1. Description of the apartment considered for the study

The building (Fig. 18) is located in Vancouver downtown; east-side, and is oriented in the North direction. The unit that is considered for the study is a 650 ft² apartment having two bedrooms; Master bedroom and children's bedroom (Bedroom 2), and is located on the 5th floor of a six storey building. The building location is characterized by relatively flat terrain and a densely populated area.

The apartment is situated in a building whose structure is characterized by reinforced concrete framework with insulated 2" × 4" steel stud wall exterior wall and 2" × 4" uninsulated steel stud partition wall. The exterior walls are mostly stucco cladding on metal lath, however, the concrete columns are covered in brick. In

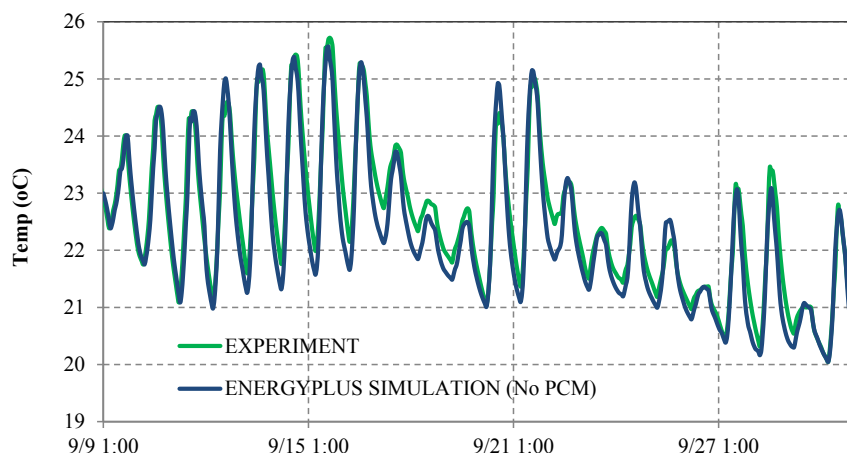


Fig. 16. Measured and simulated indoor air temperature: South building (No PCM).

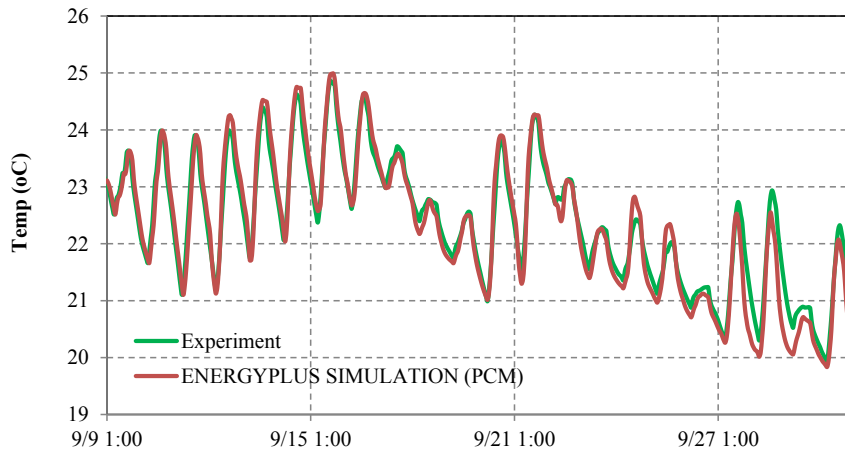


Fig. 17. Measured and simulated indoor air temperature: North building (PCM).

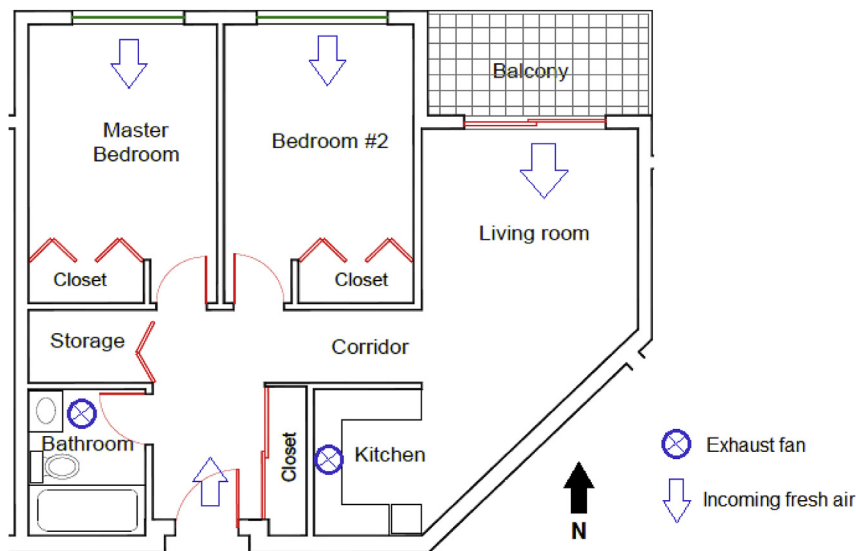


Fig. 18. Floor plan of case study apartment unit.

both cases, the interior wall finish is gypsum. All rooms bounded by the exterior have glazing and are all oriented in the same direction. The total glazing area of the living room, master bedroom and bedroom 2 are 48 ft², 25 ft² and 25 ft² respectively. All windows are aluminum framed, double glazed and air filled. Cooling and ventilation for the building is provided by corridor pressurization. The suit is intermittently depressurized by the kitchen and bathroom fan which aid further ventilation of the space. Heating however, is provided locally in each suite by electric baseboard heaters. Three baseboard heaters are located in the living room, master bedroom and bedroom 2, with electric power ratings of 2500 W, 1000 W and 1000 W respectively.

4.2. Simulation inputs

The inputs for the simulation reflect the construction and operation of the apartment unit. The building has three major zones, the living room and two bedrooms that have respective floor areas of 207 ft², and 126 ft² and height of 8 ft. All zones are separated by an insulated steel stud wall for sound proofing. The apartment is assumed to be middle apartment, as such, the floor and ceiling has similar construction; carpeted concrete. Because the

unit is the middle, all surrounding walls are assumed adiabatic besides the exterior wall. This is based on the reasoning that the adjacent apartment suites have similar indoor conditions; hence, the heat flow between apartments is insignificant. The envelope components are layered as in Table 4 with material properties adopted from ASHRAE handbook of fundamentals 2013 [52]. The windows in the bedrooms have a U-value of 3.74 W/m²K and a solar heat gain coefficient of 0.42, while that of the glazed balcony door is 3.408 W/m²K and 0.64 respectively. It is a goal of this research to investigate the influence of the glazing area on the performance of the PCM. As such, the glazing area in the master bedroom is reduced by 75% while that of bedroom 2 is simulated as-built. The interior and exterior wall surface solar emissive and absorptive properties are 0.9 and 0.7 respectively. The interior wall surface finish is medium smooth, while the rest of the interior surfaces are medium rough with inside and outside surface coefficients calculated dynamically using the simple natural and simple combined convection algorithm.

Further, the enthalpy–temperature relationship required to simulate the dynamic thermal properties of the phase change material is shown in Fig. 15. The unit is occupied by four individuals; parents and children. The occupancy is such that the

Table 4
Material properties.

Materials	Conductivity (W/m-K)	Density (kg/m ³)	Specific heat (J/kg-K)	Thickness (m)
Exterior wall				
Stucco	0.371	1795	840	0.01905
3-ply Semi-rigid Asphalt Breather Board	0.42	120	1500	0.003
Wall Air Space	Thermal Resistance: 0.15 m ² -K/W			
Semi-rigid Roxul Insulation	0.032	71	850	0.0508
Dens-Glass Gold Gypsum Sheathing	0.13	708.66	870	0.0127
Composite 2 × 4 Steel Stud R11	0.06	118.223	1048	0.089
BioPCM	0.2	235	1970	
Gypsum Drywall	0.16	625	870	0.0127
Interior partition				
Gypsum Drywall	0.16	625	870	0.0127
Composite 2 × 4 Steel Stud R11	0.06	118.223	1048	0.089
Gypsum Drywall	0.16	625	870	0.0127
Roof & floor				
Concrete	1.6	2200	850	0.0508

father goes to work during the day and the mother is a stay-at-home mum with two young children. This occupancy pattern is captured in Fig. 19. The activity level in the kitchen, bedrooms and living room are 171 W, 72 W and 108 W respectively. The clothing schedule is 2.5 clo from 10 pm to 8 am and 1.0 clo for the rest of the time. The assumption is that people like to sleep with a covering regardless of the season. The maximum occupancies of the living room, bedrooms and kitchen are 4, 2 and 1 individuals respectively. The lighting level in the Kitchen, master bedroom, bedroom 2, and living room is 40 W, 60 W, 60 W, and 100 W with radiant to visible fraction of 0.86: 0.09.

All openings including door undercuts are represented in the simulation via the EnergyPlus Airflow Network. The exterior windows and doors are dynamically controlled to open and close based on the occupant thermal comfort requirements and is achieved via the Energy Management System in EnergyPlus. The ratio of the opening area to the actual window area in the Master bedroom, bedroom 2 and Living room is 1, 0.23 and 0.5 respectively. It should be noted that the opening ratios were calculated based on building schematics. The corridor pressurization is achieved by Ideal Loads Air System that maintains the corridor at 21 °C. The kitchen exhaust is simulated to enhance the ventilation in the unit. The ON and OFF times is based on the kitchen occupancy schedule presented earlier. The simulation time step is 1 min and EnergyPlus weather file for Vancouver is used for the mild climate simulations.

4.3. Results and discussion

The analysis of the results from the numerical simulation is presented in this section. The simulation is run for a whole year and the impact of the PCM on the energy and thermal comfort is analyzed for the four seasons. It should be noted that the winter and shoulder seasons; spring and fall, show similar trend in indoor temperature profile evolutions hence, they are presented together. For that reason, only two major seasons are presented: summer and winter. It should be noted that the term “winter” is used as a loose term to describe both actual winter conditions and shoulder seasons. During the simulation, the glazing area of one of the rooms; master bedroom, was minimized to simulate a room with less solar exposure while bedroom 2 depicts a room with highly glazed façade. For further analysis, the building is reoriented from north to the west and south directions to analyze the impact of varying solar exposure. Both directions are chosen for their dominance of solar exposure in the summer and winter respectively.

4.4. Summer

This period of the year is characterized by high outdoor temperatures with focus on maintaining comfortable indoor conditions and limiting overheating. The performance of the PCM is evaluated over the month of July which is indicative of peak summer conditions. Fig. 20 and Fig. 21 show the operative temperature for the Master bedroom and bedroom 2 in the north global orientation in a typical summer week. As expected, the operative temperature in bedroom 2 has a higher peak because of the higher solar exposure and lower trough temperature because of the higher capacity for heat loss through the glazing area at night. In both cases, the thermal stabilization attributed to the PCM can slightly be seen. This is because of the minimal temperature fluctuation in both rooms which does not warrant effective charge and discharge of the PCM. Also, due to the low solar exposure with the building oriented in the north, the PCM is not frequently activated. This is reflected in the frequency of activation of the PCM, that is, how often the wall surface temperature falls within the melting temperature range of the PCM [53]. The PCM is only activated 7% and 20% in the master bedroom and bedroom 2 respectively when evaluated for the month of July. The higher activation in bedroom 2 is attributed to the higher window to wall ratio which allows for more solar gain. In fact, on average over the typical summer month, no peak attenuation is observed. However, for the few times the PCM is activated, up to 0.03 °C and 0.2 °C peak attenuation of the operative temperature is recorded for the master bedroom and bedroom 2 respectively. The relatively higher peak attenuation in bedroom 2 is expected because of the higher solar exposure; a consequence of higher glazing area. Also, the higher temperature fluctuation in bedroom 2 facilitates a better charge and discharge efficiency of the PCM.

The impact of the PCM on the temperature amplitude is also evaluated as shown in Fig. 26. It can be seen that with the PCM the temperature amplitude increases slightly. To be specific, the temperature amplitude increases by 7% and 3% in the master bedroom and bedroom 2 respectively. This occurs because the PCM acts to offset the operative temperature especially for days of interior temperatures reaching PCM activation conditions followed by days of interior conditions not reaching PCM activation conditions. It should be noted that when the relatively minimal temperature fluctuation experienced in the master bedroom amplifies the percentage amplitude increase attributed to the presence of the PCM. However, when the absolute temperature amplitude is compared the bedroom 2 shows a higher increase in the temperature amplitude which is expected because more heat is stored that could be released on consecutive days of interior temperatures reaching

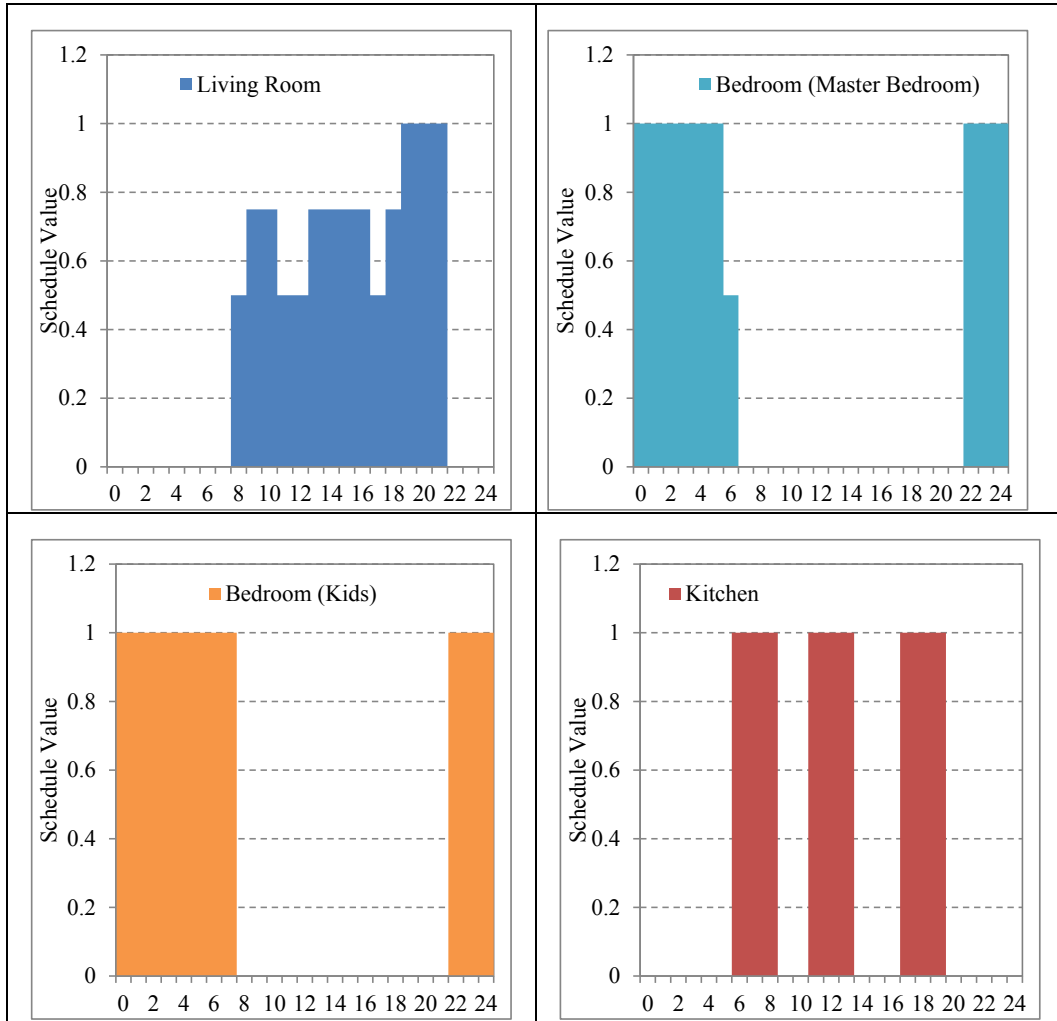


Fig. 19. Occupancy Schedule for the thermal zones in Rancho.

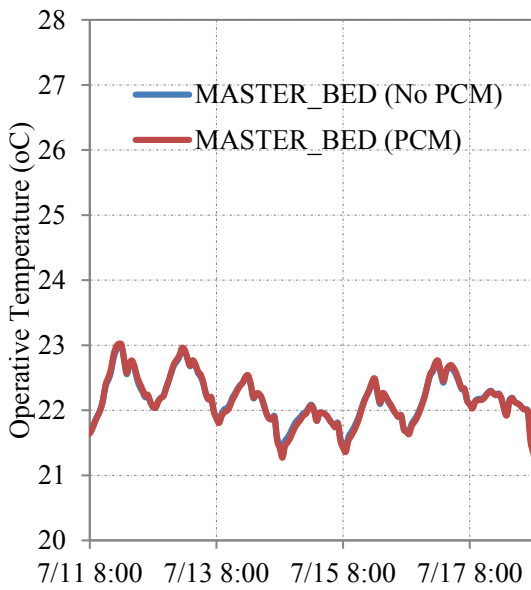


Fig. 20. Master bedroom operative temperature: North orientation.

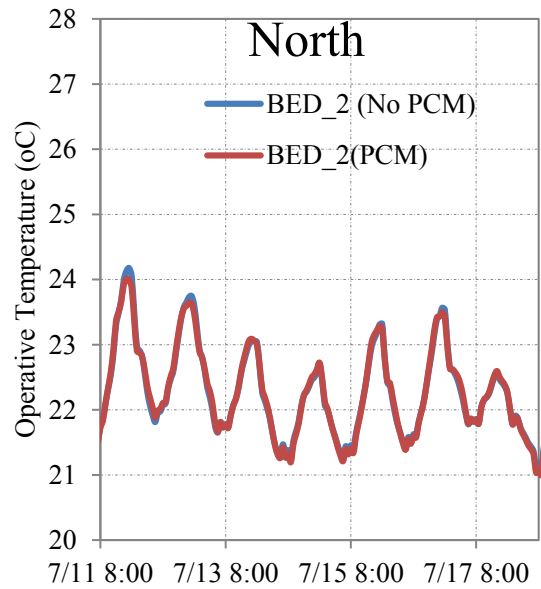


Fig. 21. Bedroom 2 operative temperature: North orientation.

PCM activation conditions and days of interior conditions not reaching PCM activation conditions.

With increased solar exposure; reorienting the glazing in the south direction, the frequency of activation increases significantly. To be specific, the PCM is active, 32% and 49% in the master bedroom and bedroom 2 respectively, for the month of July. As well, the peak temperature attenuation attributed to the presence of the PCM in the building envelope is more evident (Fig. 22 and Fig. 23). In fact, up to 0.3 °C and 0.4 °C peak temperature attenuation is calculated in the master bedroom and bedroom 2 respectively. Again, the better performance in bedroom 2 is attributed to the higher frequency of activation of the PCM due to the higher window to wall ratio that allows for more solar influx into the space with temperature peaks staying within the PCM melting temperature range.

The impact of the PCM on the temperature amplitude of the zone operative temperature is also calculated and displayed in Fig. 26. Although minimal, the temperature damping of the zone operative temperature amounts to a 3% reduction in temperature amplitude in both the master bedroom and bedroom 2. The better damping of the temperature fluctuation in the bedroom 2 is more evident when absolute values are compared. To be specific, 0.03 °C and 0.08 °C reduction in the temperature amplitude is achieved in the master bedroom and bedroom 2 respectively. Again, this is due to the elevated interior conditions while still staying within the melting temperature range of the PCM.

With an even higher solar exposure; reorienting the glazing in the west direction, the frequency of activation of the PCM further increases. To be specific, the PCM is active 54% and 64% for the total hours in a typical summer month in the master bedroom and bedroom 2 respectively. The peak attenuation and the night time temperature increase attributed to the presence of the PCM is more pronounced compared with the south orientations as shown in Fig. 24 and Fig. 25. An average peak attenuation of 0.2 °C is calculated in both the master bedroom and the bedroom 2 for the total hours of the typical summer peak month. In fact, up to 0.5 °C peak temperature attenuation is recorded in both the master bedroom and bedroom 2 respectively. The similar impact of the PCM on the interior conditions is attributed to the increased solar influx while still staying within the melting temperature range of the PCM. It is

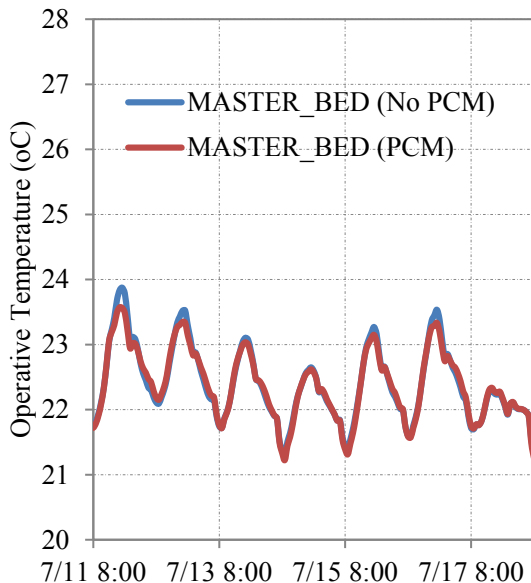


Fig. 22. Master bedroom operative temperature: South orientation.

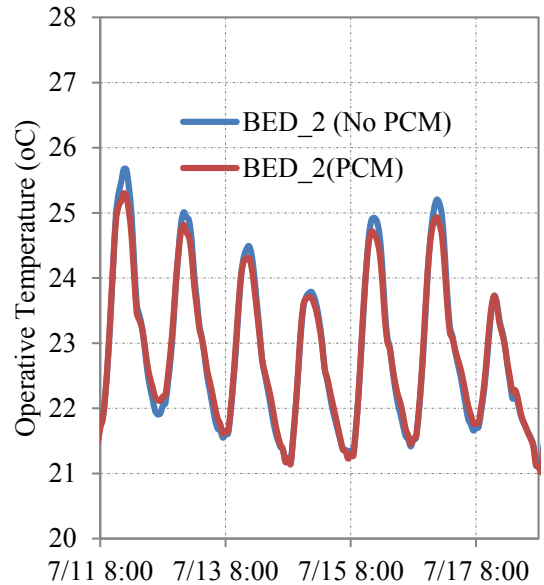


Fig. 23. Bedroom 2 operative temperature: South orientation.

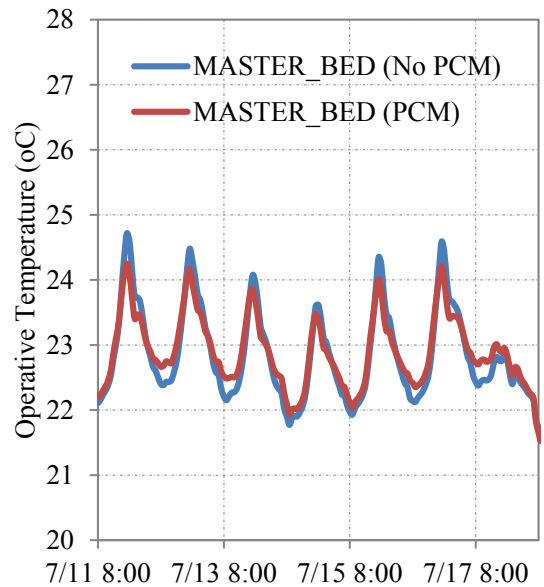


Fig. 24. Master bedroom operative temperature: West orientation.

anticipated that the performance of the PCM in the bedroom 2 will plateau faster than in the master bedroom with higher solar radiation because the chances of the operative temperature increasing beyond the melting temperature range of the PCM is high.

The PCM further dampens the temperature amplitude of the operative temperature (Fig. 26). A 14% and 9% decrease in the temperature amplitude is recorded in the master bedroom and bedroom 2 respectively when evaluated over the total hours of the typical summer month. This amounts to 0.2 °C and 0.3 °C of absolute reduction of the temperature amplitude in the master bedroom and bedroom 2 respectively. Again, a better performance is experienced in bedroom 2 because the higher solar exposure elevates the operative temperature while still staying within melting temperature range of the PCM.

The thermal comfort improvement is assessed for the number of

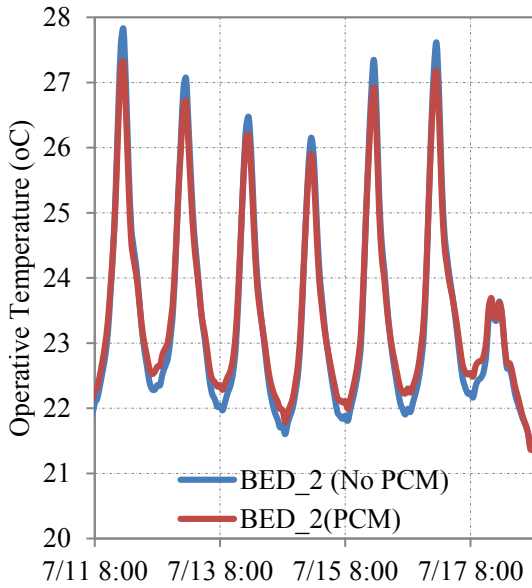


Fig. 25. Bedroom 2 operative temperature: West orientation.

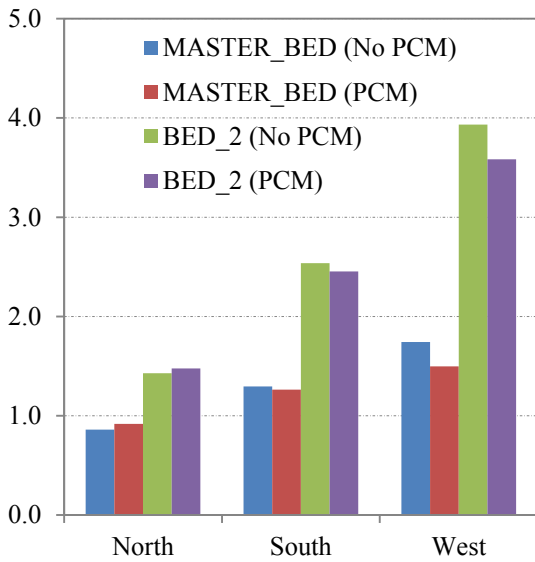


Fig. 26. Average temperature amplitude.

hours for which the percentage of people dissatisfied (PPD) is more than 10%. The 10% is borne out of ANSI/ASHRAE Standard 55 [50] as the condition that satisfies acceptable thermal environment for

Table 5
PPD improvement comparison: with and without PCM.

North		
	W/O PCM	W/PCM
Master bedroom	34	35
Bedroom 2	29	29
South		
Master bedroom	37	40
Bedroom 2	31	32
West		
Master Bedroom	26	25
Bedroom 2	19	19

general comfort. It should be noted that the thermal comfort is assessed for the times when the apartment is occupied. Table 5 shows the number of times the PPD exceeds 10% for the cases with and without PCM in both rooms.

It can be observed that the PCM has no impact on the thermal comfort. In the case of the master bedroom, the temperature does not get high enough, hence the PCM is not effectively charged during the day to warrant effective night time discharge. In bedroom 2, the temperature is relatively higher than the master bedroom; however, the temperature does not go low at night time for proper discharge. In fact, a detailed look at the operative temperature evolution for bedroom 2 suggests that the graph is symmetrical about 24 °C (Fig. 25). This may suggest incorporating a PCM with melting temperature of 24 °C for better results.

4.5. Winter and shoulder season (fall/spring)

This period of the year is characterized by cold outdoor air temperatures and hence requires mechanical system heating to maintain comfortable indoor air conditions. The focus during this period is energy and cost saving since a significant amount of energy is consumed to heat up the space. The energy usage represents near actual energy consumption since the electric baseboard heater is controlled to heat the space when the temperature drops below the setpoint during occupiable hours. The analysis of the winter and the fall is presented together since both show similar trends in indoor operative temperatures (Fig. 27 and Fig. 28). As can be seen, both have operative temperatures staying slightly above 21 °C during the occupied hours and drops lower during unoccupied hours, although lower in the winter since the outdoor conditions are more extreme. From here on the term winter is used to represent the winter and the shoulder season for clarity.

Fig. 29 and Fig. 30 show the operative temperature for the Master Bedroom and the bedroom 2 in the north global orientation in a typical winter. As observed, the operative temperature is maintained at 21 °C during occupied hours but drops below comfort conditions when the indoor temperature is allowed to float. The temperature fluctuation in the bedroom 2 is more pronounced than in the master bedroom. This is because of the higher capacity

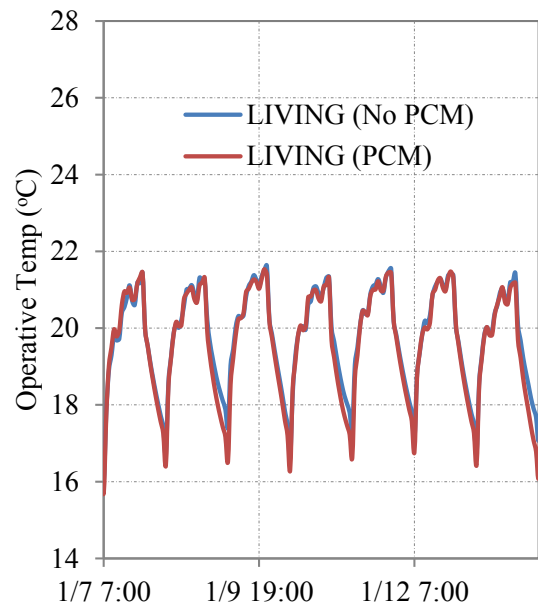


Fig. 27. Living room operative temperature: Winter.

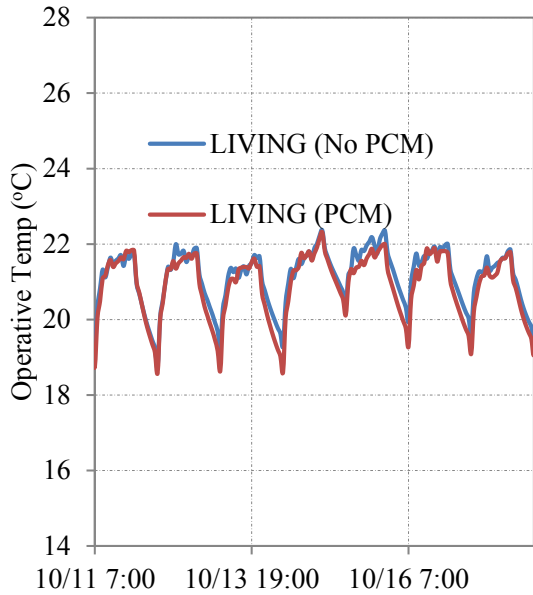


Fig. 28. Living room operative temperature: Fall.

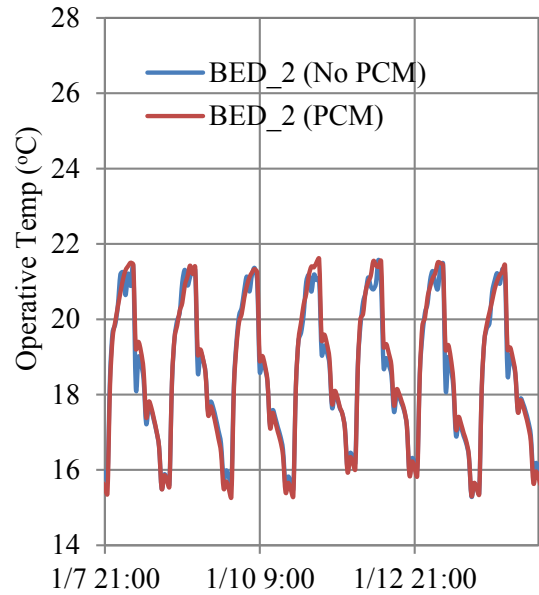


Fig. 30. Operative temperature in Bedroom 2 facing North: Winter.

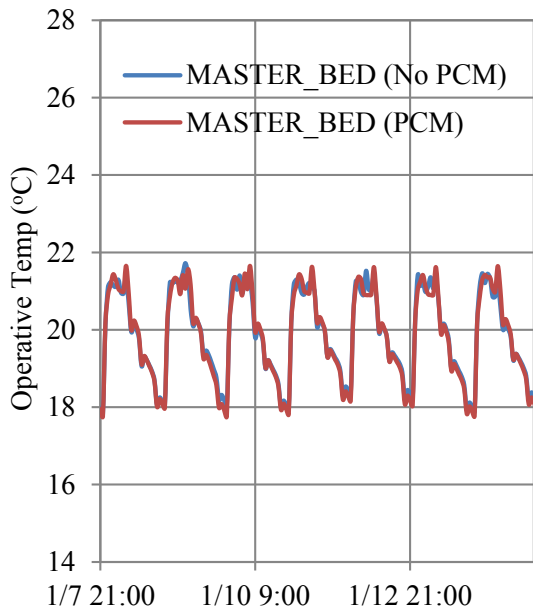


Fig. 29. Operative temperature in Master bedroom facing North: Winter.

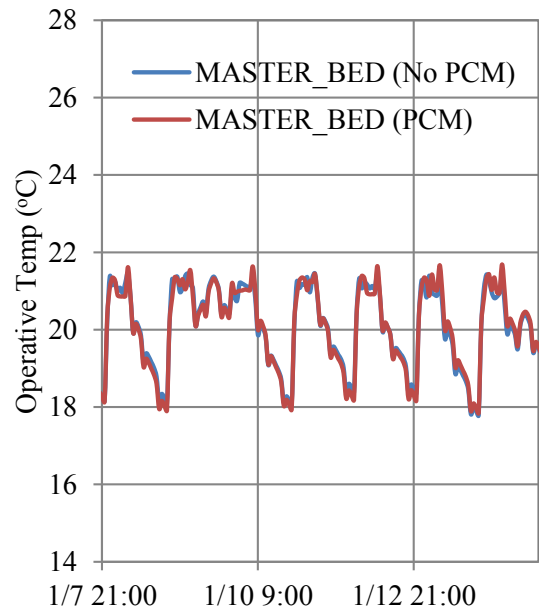


Fig. 31. Operative temperature in Master bedroom facing South: Winter.

for heat loss attributed to the relatively larger glazing area in bedroom 2. More importantly, the impact of the PCM on the interior temperature is negligible since the temperature fluctuations are well below the melting point of the PCM. This is reflected in the identical operative temperature profiles for the cases with and without PCM.

Even with the building oriented to face the south direction for higher solar exposure (Fig. 31 and Fig. 32), impact of the PCM on the temperature fluctuations is negligible. Again, this is because the indoor temperature fluctuation is below the melting point of the PCM. Notice the slight deviation of the operative temperature profile on the 2nd and 7th day of the displayed period during the free floating conditions. This deviation coincides with the rare high solar exposure encountered during the winter period (Fig. 33).

As mentioned earlier, a significant amount of energy is required for heating for the most part of this season; hence, the potential for the PCM to offset some of the heating energy is of uttermost importance. Fig. 34 shows the energy consumption for the master bedroom and bedroom 2 when the glazing is oriented in the north, south and west direction for the month of January. January is chosen to be representative of typical winter conditions as it presents the coldest month in the calendar year of Vancouver. As expected, bedroom 2 requires more energy to heat than the master bedroom because of its lower overall exterior envelope R-value. Also, by reorienting the building to directions of higher solar exposures, the total heating energy required to maintain thermal comfort is reduced as the solar exposure offsets some of the heating energy required. This is more pronounced in the south as this is the

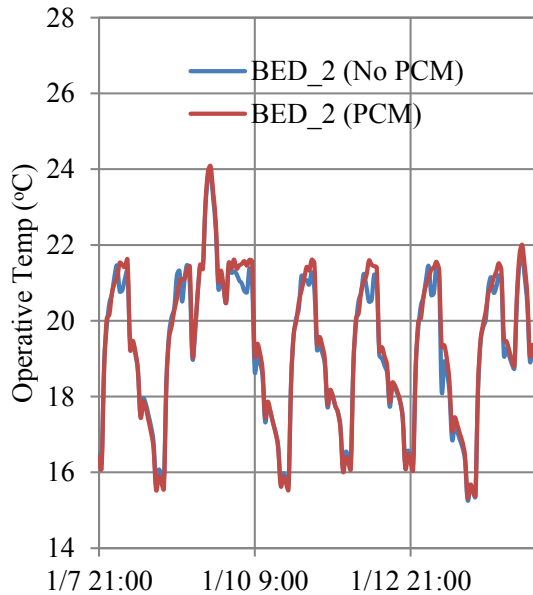


Fig. 32. Operative temperature in Bedroom 2 facing South: Winter.

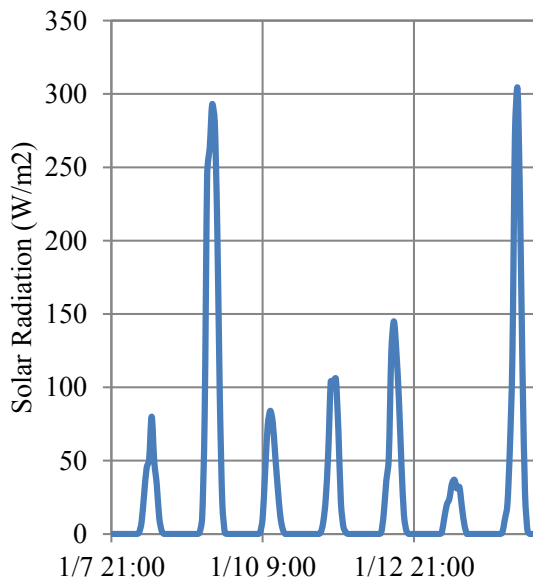


Fig. 33. Global solar radiation for the typical winter week.

direction with the most dominant solar exposure. To be specific, 7% and 1% reduction in the total heating energy attributed to the solar offset is calculated in the south and west respectively.

More important is the impact of the PCM on the heating energy demand. An energy consumption reduction of 49% and 14% is achieved in the master bedroom and the bedroom 2 respectively when the building is oriented north. In the south orientation, the PCM shows a higher impact on the heating energy consumption. In fact, an energy conservation of 57% and 25% is recorded in the master bedroom and bedroom 2 respectively. The better performance of the PCM in this direction is attributed to the higher solar exposure. With the building reoriented to the west facing direction, the heating energy reduction achieved in the master bedroom and bedroom 2 is 50% and 16% respectively. The energy reduction in all cases is attributed to the improved thermal mass of the walls with

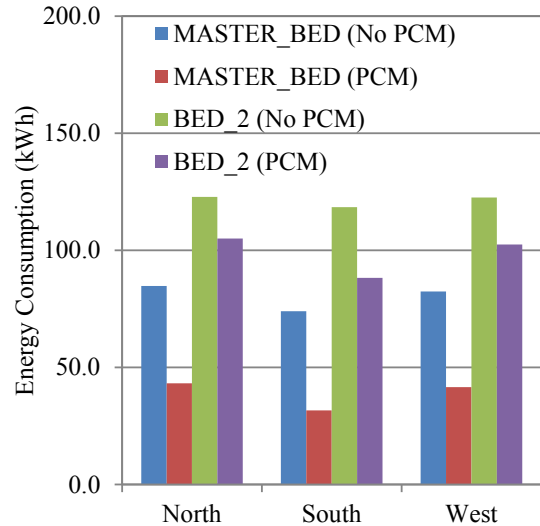


Fig. 34. Impact of PCM on the heating energy consumption in both rooms.

the PCM. Using the master bedroom as a case study, it can be noticed in Fig. 35 that the added thermal mass of the PCM acts to slow down the temperature rise of the wall surface temperature. This decreases the temperature difference across the exterior wall. Consequently, the potential for heat loss is reduced. The more pronounced energy savings in the master bedroom than bedroom 2 is attributed to the difference in the total surface area coverage of the PCM. The reduced window to wall ratio in the master bedroom allows for higher PCM coverage and an overall better improvement of the thermal mass of the walls.

From the numerical analysis, the improvement of the thermal comfort by the PCM in the summer is not evident in that the time of occurrence of peak operative temperature conditions does not coincide with the occupancy pattern. As such, despite the peak attenuation recorded of up to 0.5 °C, it is of no significance since the rooms are unoccupied. Also, the temperatures do not dip low enough to warrant efficient discharge of the stored heat during the day at night. Perhaps if the PCM is incorporated in buildings such as offices the thermal comfort benefits attributed to the incorporation of the PCM can be reaped. In such cases, the glazing area has to be optimized to allow solar influx such that the interior temperature fluctuation is within the melting temperature range of the PCM. This conclusion is drawn from observation of the trend of the results; as the building is reoriented for higher solar exposure, the benefits of the PCM in the room with higher window-to-wall ratio is more likely to plateau faster since the indoor temperature fluctuations show chances of exceeding the melting temperature range. On the contrary, the benefits of the PCM in the winter are very evident in that the added thermal mass slows down the rise of the wall temperature by absorbing some of the heat and stabilizing the wall surface temperature. This reduces the temperature gradient across the wall and the potential for heat loss. During the winter, the solar exposure as well as the heat gain is also important as this could offset some the PCM absorbed heat thereby rendering even better energy savings. This is the case when the building is reoriented in the south direction. Notice that the results from the winter and summer conflict each other in that no real thermal comfort benefit is observed whereas a significant amount of energy savings is achieved in the winter. Recall that the winter was used as a loose term to describe the winter and shoulder season which amounts to 9 months of the year requiring heating. This justifies the application of the PCM despite the ill summer results. For better

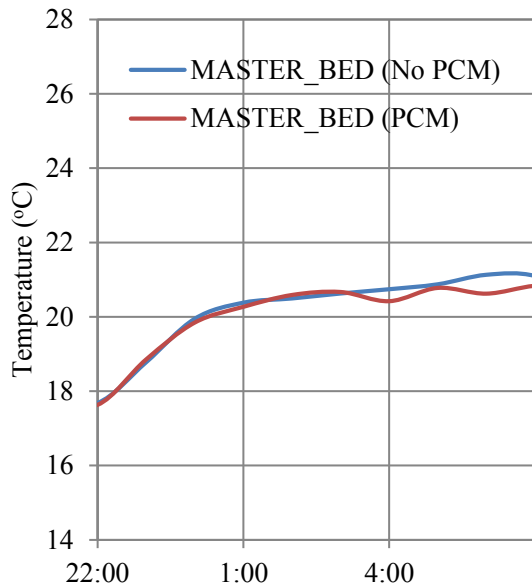


Fig. 35. Impact of PCM on the wall surface temperature in the master bedroom.

conclusion to be drawn, a cost effectiveness analysis should be carried out for pay back times.

5. Conclusion

Low inertia buildings dominate the North American residential building construction industry. Maintaining a comfortable indoor environment requires a significant amount of energy because of the unstable interior conditions. Phase change materials (PCMs) provide a means to improve the thermal inertia of these buildings. PCMs work by storing and releasing excess heat based on the boundary thermal and convective conditions. The applicability of incorporating PCMs in buildings has been researched for some time under various climates, however, there exist a gap in the thoroughness of the research techniques especially in mild climates, since more research was conducted in small huts that do not simulate actual building internal loading or with the use of numerical models that were either not validated. In this paper, the applicability of PCM in residential construction was assessed; experimentally and numerically, for its thermal comfort and energy consumption benefits with consideration to occupancy effects and changing building characteristics such as global orientation and window to wall ratio.

In the field experiment, twin buildings are used with one as reference and the other with PCM installed. For the period of testing, it was found that the PCM decreased the peak indoor air temperature by up to 0.6 °C and increased the trough temperature by 0.8 °C. This is attributed to the ability of the PCM to reverse the heat flow direction. In fact, the PCM ability to impact comfort conditions by reducing the mean radiant temperature was demonstrated in the peak wall surface temperature reduction of 1.5 °C and trough wall surface temperature increase of 1.2 °C. The numerical study was carried out for a case study building, however, the EnergyPlus simulation model was benchmarked with experimental data from the field experiment. As demonstrated, there was good agreement between the numerical simulation and the experimental data such that the discrepancies were within the tolerance limits of the indoor air measuring device. The case study building consisted of 2 bedrooms with glazing oriented in the same direction. The glazing of the one of the rooms; Master bedroom,

was modified to depict a low glazed room, while the other; Bedroom depicted a room with a highly glazed façade. It is discovered that in the summer the impact of the PCM on the thermal comfort in the space is negligible and although the more benefits of the PCM is materialized with higher solar exposure, other factors such as wind direction play significant role in materializing the benefits as the more the ventilation, the higher the efficiency of draining the stored heat. On the contrary, the impact of the PCM on the energy consumption is more pronounced. In fact, up to 63% heating energy reduction is realized in the master bedroom and 28% in bedroom 2. It was found that, with the PCM, the interior wall surface temperatures were lower thereby reducing the potential for heat loss across the exterior wall. The benefits in the winter clearly outweigh that of the summer and considering that most of the energy consumption is utilized for heating in residential applications, this attests to the applicability of PCMs in a mild climate like Vancouver.

Acknowledgment

The authors are grateful for the financial support provided by the Natural Sciences and Engineering Research Council of Canada, Canada Research Chair (CRC), Homeowner Protection Office (HPO) and the School of Construction and the Environment at the British Columbia Institute of Technology (BCIT). The contributions of Doug Horn and Wendy Simpson are also acknowledged.

References

- [1] Natural Resources Canada, Improving Energy Performance in Canada: Report to Parliament under the Energy Efficiency Act for the Fiscal Year, 2014.
- [2] R. Baetens, B.P. Jelle, A. Gustavsen, Phase change materials for building applications: a state-of-the-art review, *Energy Build.* 42 (9) (2010) 1361–1368.
- [3] M. Zhang, M.A. Medina, J.B. King, Development of a thermally enhanced frame wall with phase-change materials for on-peak air conditioning demand reduction and energy savings in residential buildings, *Int. J. Energy Res.* 29 (9) (2005) 795–809.
- [4] Y.P. Zhang, K.P. Lin, R. Yang, H.F. Di, Y. Jiang, Preparation, thermal performance and application of shape-stabilized PCM in energy efficient buildings, *Energy & Build.* 38 (10) (2006) 1262–1269.
- [5] S.D. Zwanig, Y. Lian, E.G. Brehob, Numerical simulation of phase change material composite wallboard in a multi-layered building envelope, *Energy Convers. Manag.* 69 (2013) 27–40.
- [6] M.H.M. Isa, X. Zhao, H. Yoshino, Preliminary study of passive cooling strategy using a combination of PCM and copper foam to increase thermal heat storage in building façade, *Sustainability* 2 (8) (2010) 2365–2381.
- [7] F. Ascione, N. Bianco, R.F. De Masi, F. de' Rossi, G.P. Vanoli, Energy refurbishment of existing buildings through the use of phase change materials: energy savings and indoor comfort in the cooling season, *Appl. Energy* 113 (2014) 990–1007.
- [8] T. Silva, R. Vicente, N. Soares, V. Ferreira, Experimental testing and numerical modeling of masonry wall solution with PCM incorporation: a passive construction solution, *Energy Build.* 49 (2012) 235–245.
- [9] I. Mandilaras, M. Stamatidou, D. Katsourinis, G. Zannis, M. Founti, Experimental thermal characterization of a Mediterranean residential building with PCM gypsum board walls, *Build. Environ.* 61 (2013) 93–103.
- [10] M. Ozdenef, J. Dewsbury, Dynamic thermal simulation of a PCM lined building with Energy Plus, in: Proceedings of the 5th WSEAS International Conference on Environmental and Geological Science and Engineering, 2012, July, pp. 10–12.
- [11] S.M. Silva, M.G.D. Almeida, Using PCM to Improve Building's Thermal Performance, 2013.
- [12] A. Váz Sá, R.M.S.F. Almeida, H. Sousa, J.M.P.Q. Delgado, Numerical analysis of the energy improvement of plastering mortars with phase change materials, *Adv. Mater. Sci. Eng.* 2014 (2014).
- [13] A.L. Pisello, V.L. Castaldo, F. Cotana, Dynamic Thermal-energy Performance Analysis of a Prototype Building with Integrated Phase Change Materials, 2013.
- [14] M. Saffari, A. de Gracia, S. Ushak, L.F. Cabeza, Economic impact of integrating PCM as passive system in buildings using Fanger comfort model, *Energy Build.* 112 (2016) 159–172.
- [15] A.L.S. Chan, Energy and environmental performance of building façades integrated with phase change material in subtropical Hong Kong, *Energy Build.* 43 (10) (2011) 2947–2955.
- [16] N. Zhu, S. Wang, Z. Ma, Y. Sun, Energy performance and optimal control of air-conditioned buildings with envelopes enhanced by phase change materials,

- Energy Convers. Manag. 52 (10) (2011) 3197–3205.
- [17] L. Navarro, A. de Garcia, C. Solé, A. Castell, L.F. Cabeza, Thermal loads inside buildings with phase change materials: Experimental results, *Energy Procedia* 30 (2012) 342–349.
- [18] R. Ansuini, R. Larchetti, A. Giretti, M. Lemma, Radiant floors integrated with PCM for indoor temperature control, *Energy Build.* 43 (11) (2011) 3019–3026.
- [19] F. Fiorito, Phase-change materials for indoor comfort improvement in lightweight buildings. A parametric analysis for Australian climates, *Energy Procedia* 57 (2014).
- [20] X. Shi, S.A. Memon, W. Tang, H. Cui, F. Xing, Experimental assessment of position of macro encapsulated phase change material in concrete walls on indoor temperatures and humidity levels, *Energy Build.* 71 (2014) 80–87.
- [21] P. Arce, C. Castellón, A. Castell, L.F. Cabeza, Use of microencapsulated PCM in buildings and the effect of adding awnings, *Energy Build.* 44 (2012) 88–93.
- [22] L.F. Cabeza, C. Castellon, M. Nogues, M. Medrano, R. Leppers, O. Zubillaga, Use of microencapsulated PCM in concrete walls for energy savings, *Energy Build.* 39 (2) (2007) 113–119.
- [23] A. Castell, I. Martorell, M. Medrano, G. Pérez, L.F. Cabeza, Experimental study of using PCM in brick constructive solutions for passive cooling, *Energy Build.* 42 (4) (2010) 534–540.
- [24] I. Cerón, J. Neila, M. Khayet, Experimental tile with phase change materials (PCM) for building use, *Energy Build.* 43 (8) (2011) 1869–1874.
- [25] J. Košny, E. Kossecka, Understanding a Potential for Application of Phase-Change Materials (PCMs) in Building Envelopes, *ASHRAE Trans.* 119 (1) (2013).
- [26] C. Voelker, O. Kornadt, M. Ostry, Temperature reduction due to the application of phase change materials, *Energy Build.* 40 (5) (2008) 937–944.
- [27] G. Zhou, Y. Zhang, Q. Zhang, K. Lin, H. Di, Performance of a hybrid heating system with thermal storage using shape-stabilized phase-change material plates, *Appl. Energy* 84 (10) (2007) 1068–1077.
- [28] G. Zhou, Y. Yang, H. Xu, Energy performance of a hybrid space-cooling system in an office building using SSPCM thermal storage and night ventilation, *Sol. Energy* 85 (3) (2011) 477–485.
- [29] S.H. Lee, S.J. Yoon, Y.G. Kim, J.G. Lee, The utilization of microencapsulated phase change material wallboards for energy saving, *Korean J. Chem. Eng.* 28 (11) (2011) 2206–2210.
- [30] L. Shilei, Z. Neng, F. Gouhui, Impact of phase change wall room on indoor thermal environment in winter, *Energy Build.* 38 (2005) 18–24.
- [31] A. Athienitis, C. Liu, D. Hawes, D. Banu, D. Felman, Investigation of the thermal performance of a passive solar test-room with wall latent heat storage, *Build. Environ.* 32 (5) (1997) 405–410.
- [32] X. Kong, S. Lu, J. Huang, Z. Cai, S. Wei, Experimental research on the use of phase change materials in perforated brick rooms for cooling storage, *Energy Build.* 62 (2013) 597–604.
- [33] Y.B. Seong, J.H. Lim, Energy saving potentials of phase change materials applied to lightweight building envelopes, *Energies* 6 (10) (2013) 5219–5230.
- [34] G. Zhou, Y. Zhang, X. Wang, K. Lin, W. Xiao, An assessment of mixed type PCM-gypsum and shape stabilized PCM plates in a building for passive solar heating, *Sol. Energy* 81 (11) (2007) 1351–1360.
- [35] T. Kim, S. Ahn, S.B. Leigh, Energy consumption analysis of a residential building with phase change materials under various cooling and heating conditions, *Indoor Built Environ.* 23 (5) (2014) 730–741.
- [36] E.M. Alawadhi, H.J. Alqallaf, Building roof with conical holes containing PCM to reduce the cooling load: Numerical study, *Energy Convers. Manag.* 52 (8) (2011) 2958–2964.
- [37] R. Ghedamsi, N. Settou, N. Saifi, B. Dokkar, Contribution on buildings design with low consumption of energy incorporated PCMs, *Energy Procedia* 50 (2014) 322–332.
- [38] B.M. Diaconu, M. Cruceru, Novel concept of composite phase change material wall system for year-round thermal energy savings, *Energy Build.* 42 (10) (2010) 1759–1772.
- [39] J. Košny, D.W. Yarbrough, W.A. Miller, K.E. Wilkes, E.S. Lee, Analysis of the dynamic thermal performance of fibrous insulations containing phase change materials, in: 11th International Conference on Thermal Energy Storage, 2009.
- [40] A. Pasupathy, L. Athanasius, R. Velraj, R.V. Seeniraj, Experimental investigation and numerical simulation analysis on the thermal performance of a building roof incorporating phase change material (PCM) for thermal management, *Appl. Therm. Eng.* 28 (5) (2008) 556–565.
- [41] A. Tardieu, S. Behzadi, J.J. Chen, M. Farid, Computer simulation and experimental measurements for an experimental PCM-impregnated office building, in: Proceedings of the Building Simulation 2011: 12th Conference of International Building Performance Simulation Association, Vol. 1, 2011, November, pp. 56–63.
- [42] A.G. Entrop, H.J.H. Brouwers, A.H.M.E. Reinders, Experimental research on the use of micro-encapsulated phase change materials to store solar energy in concrete floors and to save energy in Dutch houses, *Sol. Energy* 85 (5) (2011) 1007–1020.
- [43] S. Behzadi, M.M. Farid, Experimental and numerical investigations on the effect of using phase change materials for energy conservation in residential buildings, *HVAC&R Res.* 17 (3) (2011) 366–376.
- [44] W. Qureshi, N. Nair, M. Farid, Impact of energy storage in buildings on electricity demand side management, *Energy Conserv. Manag.* 52 (2011) 2110–2120.
- [45] F. Kuznik, J. Virgone, K. Johannes, In-situ study of thermal comfort enhancement in a renovated building equipped with phase change material wallboard, *Renew. Energy* 36 (5) (2011) 1458–1462.
- [46] M. Ahmad, A. Bontemps, H. Sallée, D. Quenard, Thermal testing and numerical simulation of a prototype cell using light wallboards coupling vacuum isolation panels and phase change material, *Energy Build.* 38 (6) (2006) 673–681.
- [47] F. Kuznik, J. Virgone, J.J. Roux, Energetic efficiency of room wall containing PCM wallboard: A full-scale experimental investigation, *Energy Build.* 40 (2) (2008) 148–156.
- [48] A. Bontemps, M. Ahmad, K. Johannès, H. Sallée, Experimental and modelling study of twin cells with latent heat storage walls, *Energy Build.* 43 (9) (2011) 2456–2461.
- [49] F. Tariku, Y. Simpson, S. Pedram, D. Horn, et al., Development of a Whole-Building Performance Research Laboratory for Energy, Indoor Environment and Building Envelope Durability Study, Proceedings from ZEMCH 2013 International Conference. Miami, FL (2013).
- [50] ASHRAE 55, Thermal Environment Conditions for Human Occupancy, American Society of Heating, Refrigerating and Air-Conditioning Engineers, 2010.
- [51] P.C. Tabares-Velasco, C. Christensen, M. Bianchi, Verification and validation of EnergyPlus phase change material model for opaque wall assemblies, *Build. Environ.* 54 (2012) 186–196.
- [52] ASHRAE Handbook – Fundamentals, American Society of Heating, Refrigeration and Air-conditioning Engineers, Inc., Atlanta, GA, 2013.
- [53] G. Evola, L. Marletta, F. Sicurella, A methodology for investigating the effectiveness of PCM wallboards for summer thermal comfort in buildings, *Build. Environ.* 59 (2013) 517–527.